5176 J. Med. Chem. 2009, 52, 5176–5187
DOI: 10.1021/jm900365v

Journal of Medicinal Chemistry Article

Synthetic Analogue of Rocaglaol Displays a Potent and Selective Cytotoxicity in Cancer Cells: Involvement of Apoptosis Inducing Factor and Caspase-12

Frédéric Thuaud,[†] Yohann Bernard,[†] Gulen Turkeri,[‡] Ronan Dirr,[†] Geneviève Aubert,[§] Thierry Cresteil,[§] Aurélie Baguet,[∥] Catherine Tomasetto,[∥] Yuri Svitkin,[⊥] Nahum Sonenberg,[⊥] Canan G. Nebigil,[‡] and Laurent Désaubry*[,†]

[†]*Therapeutic Innovation Laboratory, UMR7200, CNRS/Université de Strasbourg, Illkirch, France,* [‡]*Institut de Recherche de l'Ecole de Biotechnologie de Strasbourg, FRE 3211, CNRS/Université de Strasbourg, Illkirch, France,* [§]*Institut de Chimie des Substances Naturelles, CNRS UPR 2301, Gif-sur-Yvette, France,* [∥]*Institut de Génétique et de Biologie Moléculaire et Cellulaire, U 596 INSERM/UMR7104 CNRS/Université de Strasbourg, Illkirch, France, and* [⊥]*Department of Biochemistry, McGill Cancer Centre, McGill University, Montreal, QC H3G1Y6, Canada*

Received March 23, 2009

Flavaglines constitute a family of natural anticancer compounds. We present here **3** (FL3), the first synthetic flavagline that inhibits cell proliferation and viability ($IC_{50} \approx 1$ nM) at lower doses than did the parent compound, racemic rocaglaol. Compound **3** enhanced doxorubicin cytotoxicity in HepG2 cells and retained its potency against adriamycin-resistant cell lines without inducing cardiomyocyte toxicity. Compound **3** induced apoptosis of HL60 and Hela cells by triggering the translocation of Apoptosis Inducing Factor (AIF) and caspase-12 to the nucleus. A fluorescent conjugate of **3** accumulated in endoplasmic reticulum (ER), suggesting that flavaglines bind to their target in the ER, where it triggers a cascade of events that leads to the translocation of AIF and caspase-12 to the nucleus and probably inhibition of eIF4A. Our studies highlight structural features critical to their antineoplastic potential and suggest that these compounds would retain their activity in cells refractory to caspase activation.

Introduction

Flavaglines are a family of natural compounds extracted from Asian plants of the genus *Aglaia*.[1,2] King et al. isolated the first flavagline, rocaglamide, in 1982 on the basis of its potent in vivo activity against murine P388 lymphocytic leukemia.[3] Since then, many other flavaglines, such as rocaglaol or silvestrol, have been isolated, mainly by the pharmacognosy laboratories of Kinghorn, Pezzuto, and Proksch.[1,2] These cyclopenta[*b*]benzofurans have been shown to inhibit the proliferation of tumor cells in a low nanomolar range, either by cytostatic[4−8] or cytotoxic effects,[9−14] depending on compound and cell line.

Unlike other anticancer drugs, flavaglines are extremely effective against cancer cell lines without displaying any significant toxicity on normal cells, such as human umbilical vein endothelial cells (HUVEC[a]),[15] intestinal epithelial cell line IEC18,[6] normal peripheral blood lymphocytes, and bone marrow stem cells.[14] Moreover, these compounds do not induce any loss of body weight or any other sign of toxicity in mice.[7] Flavaglines have been reported to induce apoptosis via the intrinsic pathway.[12,16]

Flavaglines strongly activate the stress-response mitogen-activated protein kinase p38 in leukemia and colorectal tumor cell lines.[6,14] In addition, they potently inhibit protein synthesis but not DNA nor RNA synthesis in several cancer cell lines, suggesting that their cytostatic properties involve inhibition of protein synthesis.[5,7,8]

Pezzuto and colleagues have shown that a naturally occurring flavagline delays for 23 days the growth of a human breast cancer cell line (BC1) in athymic mice.[7] The unique biological profile of flavaglines has attracted considerable interest these last 10 years, but the studies of their structure−activity relationships were limited to natural compounds because of the difficulty to synthesize them. The specificity of flavaglines' cytotoxicity toward cancer cells coupled to a unique array of biological activity and an unknown mode of action prompted us to pursue the exploration of their structure−activity relationships and their therapeutic potential in the treatment of cancer.

Herein we report on the preparation and biological evaluation of rocaglaol analogues FL2−4 (**2**−**4**), fluorescent probe **5**, and affinity ligand **6** (Figure 1). This study led to the identification of a synthetic compound displaying an enhanced in vitro cytotoxicity compared with racemic rocaglaol **1**. We also present a model that accounts for the mechanism by which flavaglines induce apoptosis in cancer cells.

Chemistry

The structural requirements for the antiproliferative capacity tested upon cancer cell lines have been limited to flavaglines extracted from plants. Flavaglines are cyclopenta-[*b*]benzofuran lignans substituted by two aryl groups with poorly explored structure−activity relationships. Because

*To whom correspondence should be addressed. Phone: 33-390-244-141. Fax: 33-390-244-145. E-mail: desaubry@chimie.u-strasbg.fr.

[a] Abbreviations: HUVEC, human umbilical vein endothelial cells; MTS, 3-(4,5-dimethylthiazol-2-yl)-5-(3-carboxymethonyphenol)-2-(4-sulfophenyl)-2*H*-tetrazolium; PI, propidium iodide; FACS, fluorescence-activated cell sorting; Z-VAD-FMK, benzyloxycarbonyl-Val-Ala-Asp(OMe)-fluoromethylketone; ER, endoplasmic reticulum; MLN51, metastatic lymph node 51 protein; FMRP, fragile X mental retardation protein; AIF, apoptosis inducing factor; DAPI, 4′-6-diamidino-2-phenylindole; ATAD, benzyloxycarbonyl-Ala-Thr-Ala-Asp(OMe)-fluoromethylketone; casp-12, caspase-12; MTF, molecular target of flavaglines.

 Published on Web 08/05/2009

rocaglaol is particularly active and can be conveniently synthesized by the approach developed by Dobler and collaborators, we selected this flavagline as a reference compound to examine the effects of substitutions on these two aryl moieties. The synthesis of racemic rocaglaol (**1**) and its analogues **2**−**4** started with the Michael addition of benzofuranones **7** to cinnamaldehyde **8**, resulting in a mixture of adducts **9** and **10** (2:3 ratio) that were separated by silica gel chromatography (Scheme 1).[17] Formation and ring closure of cyanohydrins **11** afforded the cyclopenta[*b*]benzofurans **12**. Subsequent deprotection and stereospecific reduction of the ketones by $Me_4NBH(OAc)_3$ provided flavaglines **1**−**4**.

To identify the intracellular localization of the molecular target of flavaglines, we conjugated flavagline **17** to *N*,*N*-dimethyl-7-aminocoumarin **18** through a linker. We selected this blue fluorescent dye because it displays suitable photophysical properties for fluorescence microscopy, it easily penetrates into cells, and it does not localize preferentially in a subcellular compartment.[18] The synthesis of flavagline **17** was performed according to the approach developed by Porco and colleagues[19] (Scheme 2). Photocycloaddition [3 + 2] of hydroxyflavone **13** with methyl cinnamate **14**, followed by an acyloin rearrangement, gave a mixture of inseparable diastereomers **16**. Reduction by $Me_4NBH(OAc)_3$, HPLC purification and saponification afforded the expected racemic flavagline **17**.

Coupling of coumarin **18** with mono-Boc protected diamine **19**[20] was mediated by ECDI/HOBT. Subsequent deprotection by TFA in CH_2Cl_2 at room temperature afforded the amine **20** (72% yield for two steps). ECDI/HOBT-mediated coupling with **17** afforded the fluorescent probe **5** in a 22% yield. We also prepared unconjugated coumarin **21** by acylation of **20**, for use as a negative control in confocal microscopy studies.

To detect the molecular target of flavaglines by pull-down experiments, we conjugated the carboxylic derivative of **3** onto Affi-Gel 10 through a linker. Coupling of **23** with amino linker **24** was mediated by ECDI/HOBT in CH_2Cl_2 at 0 °C. Initial attempts to reduce azide **25** to amine **6** with triphenylphosphine or 1,3-propanedithiol were unsuccessful due to the formation of many side-products. Finally, the use of thiophenol and $SnCl_2$ according to Fuch's method[21] allowed us to prepare amine **6** in 75% yield, which was quantitatively conjugated to Affi-Gel 10 (Scheme 3).

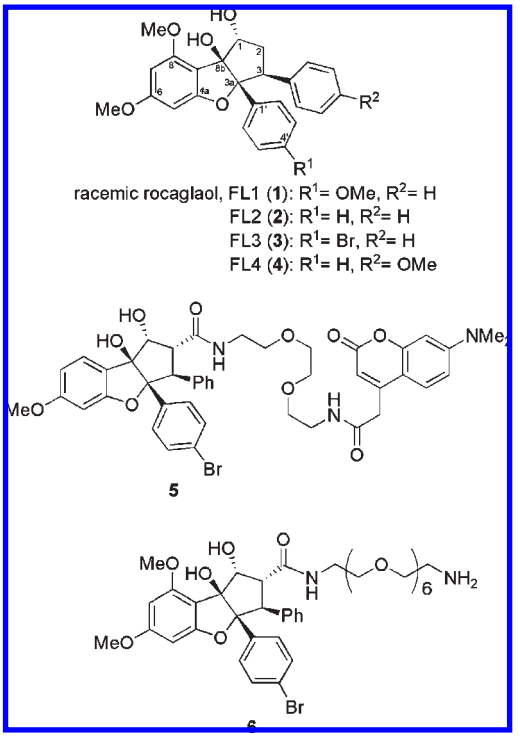

Figure 1. Structures of **1** (racemic rocaglaol, FL1), analogues **2**−**4** (FL2−4), fluorescent probe **5**, and affinity ligand **6**.

Biological Results

In Vitro Cell Growth Inhibition Assay. The antiproliferative capacities of racemic rocaglaol (**1**) and its analogues **2**−**4** were determined on a variety of human cancer cell lines from nasopharynx (KB), breast (MCF7, MCF7R), colon (HCT116 and HCT15), liver (HepG2), and neutrophil (HL60)-derived neoplasms by the MTS assay after a 72 h treatment. As shown in Table 1, **1** reduced the cell proliferation and viability at lower doses (in the low nanomolar range) than the anticancer drugs doxorubicin, cisplatin, and camptothecin on a panel of human cancer cell lines. Removing a methoxy group (R^1 = H) decreased potency more than 3 orders of magnitude (compound **2**, Table 1). Conversely, the replacement of this methoxy group by a

Scheme 1[a]

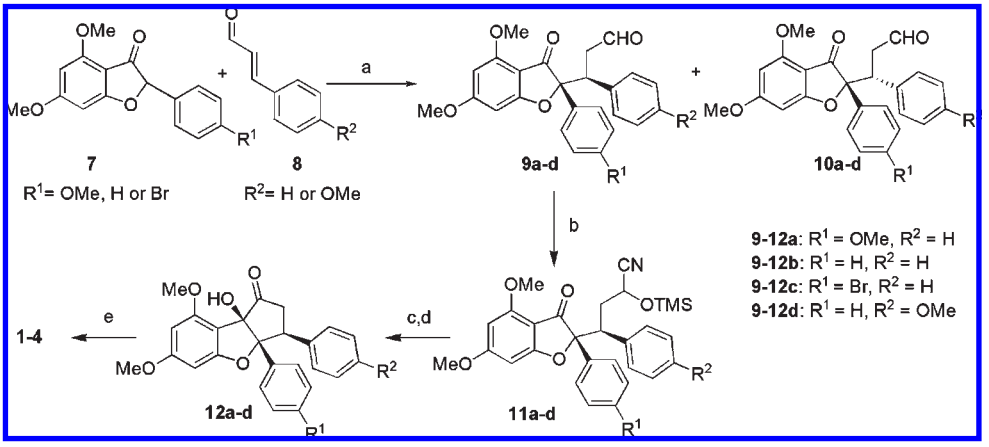

[a] Reagents and conditions: (a) triton B, THF, rt, 1 h; (b) TMSCN, ZnI_2, MeCN, benzene, rt, 12 h ; (c) LDA, THF, −78 °C, 1 h; (d) K_2CO_3, MeOH, rt, 15 min; (e) $Me_4NBH(OAc)_3$, MeCN, AcOH, rt, 18 h.

Scheme 2[a]

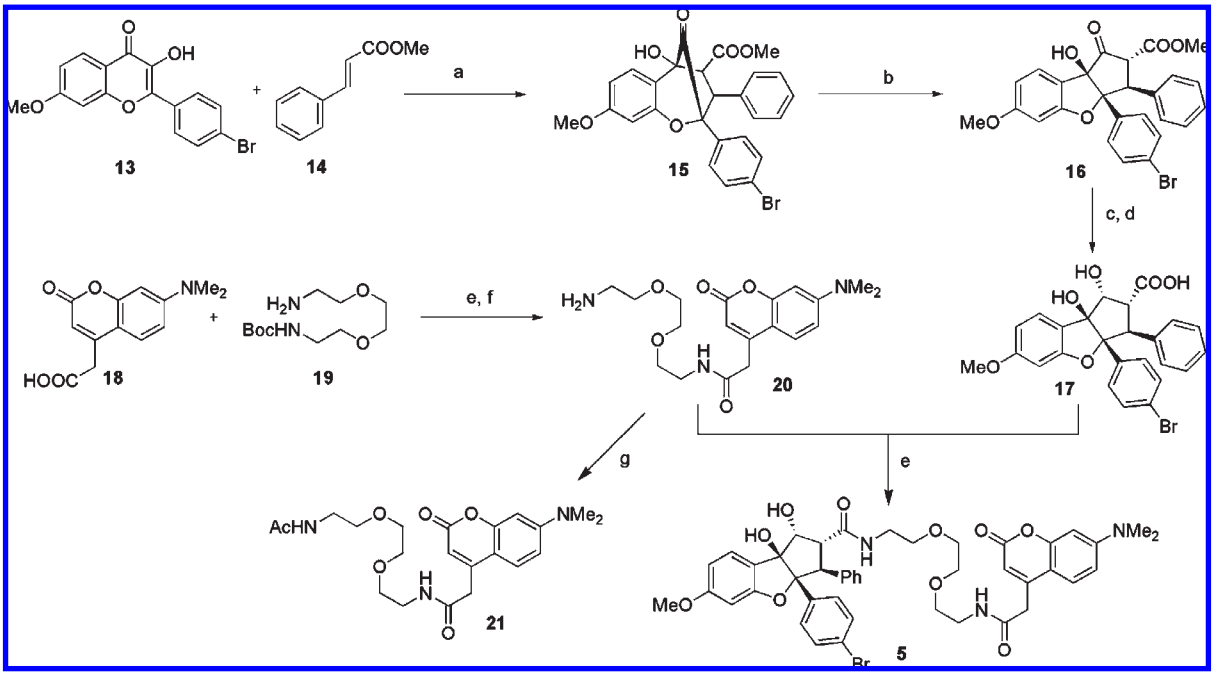

[a] Reagents and conditions: (a) hν, CH_2Cl_2-MeOH, 0 °C, 15 h; (b) MeONa, MeOH, 60 °C, 20 min; (c) $Me_4NBH(OAc)_3$, CH_3CN; (d) KOH, MeOH, 45 °C, 12 h; (e) ECDI, HOBT, DIPEA, CH_2Cl_2, rt, 12 h; (f) TFA, CH_2Cl_2, rt, 12 h; (g) Ac_2O, Et_3N, CH_2Cl_2, rt.

Scheme 3[a]

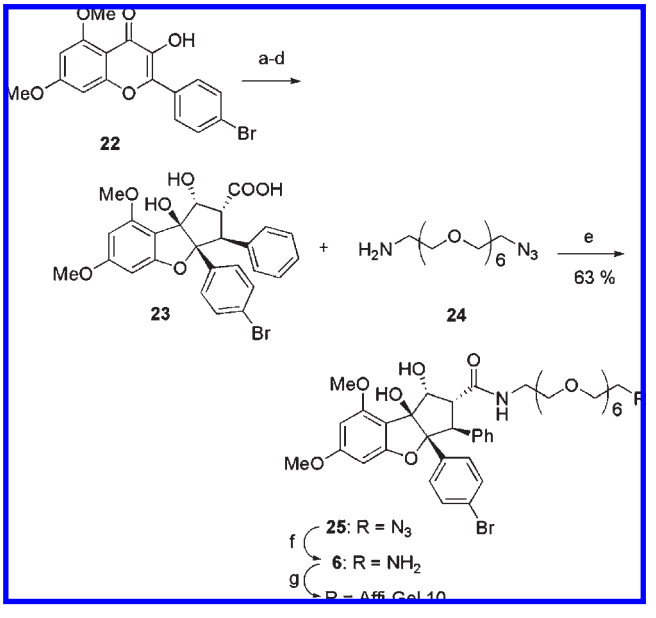

[a] Reagents and conditions: (a) hν, CH_2Cl_2−MeOH, 0 °C, 30 h; (b) MeONa, MeOH, 60 °C, 20 min; (c) $Me_4NBH(OAc)_3$, CH_3CN; (d) KOH, MeOH, 45 °C, 12 h; (e) ECDI, HOBT, DIPEA, CH_2Cl_2, rt, 12 h; (f) PhSH, $SnCl_2$, Et_3N, CH_3CN, rt, 3 h (75%); (g) Affi-Gel 10, Et_3N, CH_3CN, rt, 12 h (100%).

bromine atom (R^1 = Br) improved the cytotoxicity against all of these cancer cell lines (compound **3**). The rank of activity (H ≪ MeO < Br) suggests a preference for a hydrophobic substituent in this para position. Introduction of a methoxy on the other phenyl moiety (R^2 = OMe) was detrimental for cytotoxicity (compare **4** with **2**).

Interestingly, the cytotoxicity potential of **1** and **3** was retained in the two cell lines HCT15R and MCF7R that have developed resistance to chemotherapy by expressing the P-glycoprotein (P-gp), a plasma membrane protein also named "permeability glycoprotein" and encoded by the multidrug resistance (MDR1) gene (see Table 1). This was further confirmed by the direct measurement of drug efflux from MCF7R cells in the presence of 0.1−1 μM **1**−**4**. Indeed, under flavaglines **1**−**4** the efflux of rhodamine 123 from cells was unchanged, demonstrating the lack of interaction between flavaglines and P-gp.

Combination of Flavaglines and Doxorubicin on Cancer Cell Line. Flavaglines have been shown to sensitize therapy-resistant leukemic T cells to apoptosis induced by TNF-α, cisplatin, and γ-irradiation,[22] but their possible potentiating effects upon anthracycline-induced cytotoxicity have not been investigated. Because of the critical need to develop efficient therapies for hepatocellular carcinoma,[23] we selected HepG2 cells to investigate whether **1** and **3** could potentiate doxorubicin-induced apoptosis. Note that these slowly growing cells display a low sensitivity toward clinically used anticancer drugs (Table 1). Gratifyingly, both **1** and **3** exhibited additive cytotoxic effects with doxorubicin (Figure 2). As expected, this enhancement of doxorubicin cytotoxicity was more pronounced with **3** than **1**.

Flavaglines are Not Cardiotoxic. Many anticancer drugs, such as cisplatin, imatinib mesylate (Gleevec), and trastuzumab (Herceptin) are cardiotoxic.[24,25] This cardiotoxicity is even a major limitation to the use of anthracyclines in clinics. Therefore, one of the major challenges in anticancer therapy is to develop therapeutic agents that do not compromise heart function. This prompted us to investigate whether **1** and **3** are cytotoxic in H9c2 cardiomyoblast cell lines. These cardiomyoblasts derived from rat heart represent an established model to study cardiotoxicity in vitro.[26] Cell cycle progression and apoptosis were measured in H9c2 cells treated with **1**, **3** doxorubicin, or their vehicle, labeled with annexin and propidium iodide (PI), and analyzed by

Table 1. Inhibition of Cell Proliferation by Flavaglines **1**−**4** on Various Human Cancer Cell Lines (IC_{50}, nM)[a]

cell lines	**1**	**2**	**3**	**4**	doxorubicin	docetaxel	cisplatin	camptothecin	vinblastine
KB	2	2500	< 1	> 10000	1	0.2	2200	38	0.8
MCF7	4	10000	1	NI	12	NI	4800	10	4.6
MCF7R	4	10000	< 1	> 10000	58	NI	3100	3	NI
HCT116	6	6000	< 1	> 10000	6	0.5	2700	2	1.3
HCT15	6	8000	1	NI	81	13	2900	3	10
HepG2	70	> 10000	4	NI	240	NI	> 10000	455	NI
HL60	3	6000	< 1	> 10000	13	0.5	5900	6	1

[a] IC_{50} values were determined from dose−response curves performed in duplicate according to methods described under Experimental Section. NI: noninhibiting at the highest concentration tested.

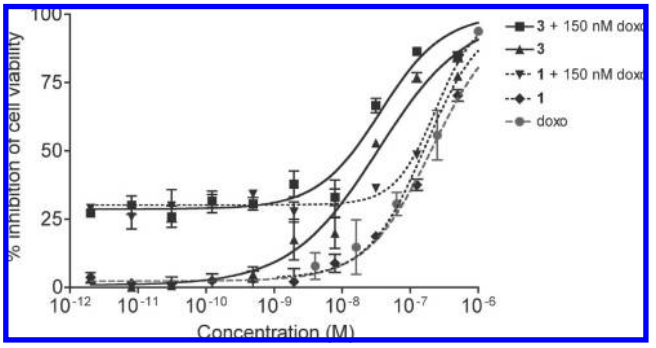

Figure 2. Inhibition of cell proliferation of HepG2 cells exposed to **1** and **3** with or without doxorubicin. HepG2 cells were treated with **1** (♦) or **3** (▲) alone or with 150 nM doxorubicin (**1**: ▼, **3**: ■) for 72 h, and cell proliferation was measured by MTS assay. Experiments were performed in duplicate ($n = 3$).

fluorescence-activated cell sorting (FACS). Additionally, cell viability was also assessed by the MTS assay. Remarkably, incubation of H9c2 cells with 0.5−50 nM of **1** or **3** for 24 h did not induce apoptosis, indicating that flavaglines are not deleterious to H9c2 cardiomyocytes (Figure 3a). On the opposite, doxorubicin (1 μM) treatment for 24 h induced a 3-fold increase in cell death. No clear sign of apoptosis or alteration of cell viability were observed after 48 and 72 h of treatment with **3** (20 nM; Figures 3b,c). Next we examined general toxicity in mice: **3** was administered i.p. twice a day for four consecutive days at a dose of 0.1 mg/kg, body weights were measured once a day for 13 days. No overt sign of acute toxicity, such as diarrhea and body weight loss, was observed (Figure 3d).

Flavaglines Block HL60 Cells in G2/M Phase. To investigate the effect of flavaglines on cell cycle progression and apoptosis, HL60 cells were treated for 48 h in a medium containing varying concentrations of **1** and **3**. A similar experiment was performed with 20 μM doxorubicin as a positive control. DNA content was determined by flow cytometry of PI-stained cells (Figure 4a). Incubation of HL60 cells for 48 h with **1** (200 nM) or **3** (20 nM) resulted in the accumulation of cells in the G2/M phase of the cell cycle. Note that treatment of cells with 1% DMSO alone (vehicle control) had no effect on cell cycle profile compared with untreated controls. An increase in the percentage of total cells in the G0-G1 peak, characteristic of apoptotic cells, was observed progressively with both **1** and **3**.

Compound 3 Induces Apoptosis in HL60 Cells Independently of Caspases 3/7. We determined by FACS analysis apoptosis of HL60 cells after **1** or **3** treatment (Figure 4b). After 72 h of treatment with **3** (20 nM), 43% of HL60 cells were killed, indicating that apoptosis is the main cell death pathway involved in the cytotoxicity of **3** in these cells. Next we tested whether **1** and **3** induced apoptosis in a caspase-dependent manner. To address this question we investigated caspase 3/7, 8, and 9 activities in HL60 cells treated for 48 h with **1** or **3**. As shown in Figure 4c and Supplementary Figure S1, neither **1** nor **3** treatment significantly activated caspases 3/7 in a concentration-dependent manner, suggesting that caspase activation seen after treatment with **1** or **3** is a consequence of **1** or **3**-induced apoptosis rather than a direct effect on caspase activity. In comparison, 1 μM doxorubicin increased caspase 3/7 activity by 14-fold. Moreover, no cleavage of the upstream caspase cascade precursors (caspases 8 and 9) was detected after treatment with **3** in the same cells (Supplementary Figure S2). Taken together, these data suggest that **1** and **3** induce apoptosis in HL60 cells without acting directly on caspase 3/7.

Inhibitors of Caspases, Necroptosis, and Autophagy do not Block the Cytotoxicity of 3 in HL60 Cells. To further characterize molecular mechanisms behind cytotoxicity of **3** in cancer cells, we examined whether this effect could be blocked by the broad-spectrum caspase inhibitor Z-VAD-FMK, and also by 3-methyladenine and necrostatin-1, which respectively inhibit autophagy and necroptosis.[27,28] The antiproliferative activity of both **1** and **3** was unchanged under cotreatment with these inhibitors (Figure 4d and Supplementary Figure S3), which confirms that apoptosis is the main mechanism by which **3** induces the death of HL60 cells and that it does not involve caspases.

Compound 3 does not Inhibit the Proteasome. Some drugs like bortezomib (MG132) exert their cytotoxic effects through the inhibition of protease activities mediated by the proteasome.[29] To test whether **1** and **3** could act on the proteasome, lysates of HL60 cells were treated with **1** or **3** and their capacity to modulate in vitro chymotrypsin- or trypsin-like activities of these cell lysates was measured. Neither **1** (20−200 nM) nor **3** (2−20 nM) was capable of eliciting a reduction of proteasome activity, in contrast with bortezomib (100 nM), which was used as positive control for assessing chymotrypsin-like activity of the proteasome (Supplementary Figure S4).

Compound 3 Inhibits Protein Synthesis, Independently from eIF2-α Phosphorylation. Rocaglaol (nonracemic **1**) has been reported to inhibit protein translation.[8] Given the importance of translation in cell growth and tumorigenesis, we checked whether **3** could exert its cytotoxic effect by inhibition of protein synthesis. Using an in vitro-based translation assay of capped and polyadenylated luciferase mRNA in a rabbit reticulocyte lysate (Figure 5A), we observed that **3** inhibited translation in this assay at micromolar concentrations, doses that are 1000 times higher than cytotoxic doses for cancer cells.

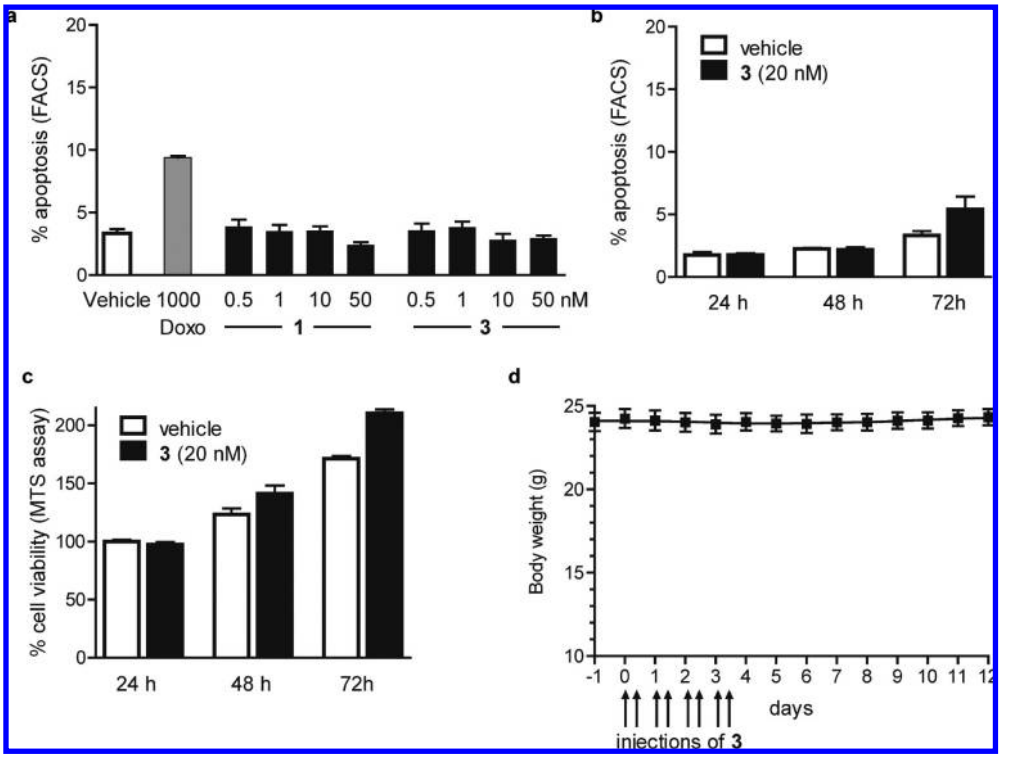

Figure 3. Flavagline **3** is not cardiotoxic. (a) Neither **1** nor **3** induced apoptosis in H9c2 cardiomyocytes. H9c2 cells were treated with **1** and **3** or their vehicle for 24 h and then labeled with annexin V and PI for FACS analysis. Remarkably, incubation of H9c2 cells with different concentrations of flavagline for 24 h did not alter the apoptotic cell number as compared to the vehicle treatment, indicating that flavaglines do not display any adverse sign of apoptosis in H9c2 cardiomyocytes. (b) Compound **3** (20 nM) does not induce apoptosis of H9c2 cells after 24, 48, and 72 h. (c) Compound **3** (20 nM) does not alter cell viability of H9c2 cells. Cells were treated as previously and viability was assessed by MTS assay. (d) Flavagline **3** does not induce loss of body weight in mice. Compound **3** was administered i.p. twice a day for four consecutive days at a dose of 0.1 mg/kg to male B6 mice and body weights were measured once a day for 13 days.

Next, we examined whether **3** induced the phosphorylation of the α-subunit of the eukaryotic initiation factor 2 (eIF-2α), a key regulator of protein synthesis. Its phosphorylation results in inhibition of translation initiation and the formation of cytoplasmic aggregates called stress granules.[30] Moreover, abrogation of eIF-2α phosphorylation causes malignant transformation of NIH 3T3 cells.[31] Using an antibody specific for phosphorylated eIF2-α, we found that eIF2-α phosphorylation was unaffected in HeLa cells treated for 1 h with **3** (100 and 500 μM; Figure 5B). Arsenite, which is known to induce eIF2-α phosphorylation, was used as a positive control.

Stress granules are storage regions for untranslated mRNAs that appear in the cytoplasm of cells under stress conditions. To examine whether **3** induces stress granule formation, immunofluorescence analyses were performed with stress granules markers such as MLN51 and FMRP proteins.[32,33] Interestingly, **3** treatment induced the formation of stress granules in HeLa cells at doses with which it inhibits protein synthesis (concentrations of **3** > 10 μM) and that are 1000 times higher than the effective cytotoxic concentrations (Figure 6).

The recent discovery that flavaglines inhibit the eukaryotic translation initiation factor 4A (eIF4A) prompted us to examine by a pull-down experiment whether an immobilized flavagline binds to this factor.[34] First, derivative **6** was immobilized onto an Affi-Gel 10 matrix through a linker. Pull down assays did not reveal any interaction between **6** and eIF4A (Supplementary Figure S5), suggesting that flavaglines might not physically interact with eIF4A.

Fluorescent Probe 5 Accumulates in Endoplasmic Reticulum of Cancer Cells. To identify the intracellular localization and therefore the potential molecular target of flavaglines, we examined the cellular uptake of **5** in HeLa cells by fluorescence microscopy. This probe displayed a cytotoxicity against HL60 cells with an IC_{50} of 130 nM, indicating that it maintained a critical proportion of the activity of **3**. Living HeLa cells were incubated with this fluorescent probe and a specific signal was localized in the cytoplasm (Figure 7), thus excluding the nucleus, Golgi apparatus, endolysosomes, and the plasma membrane as the locus of the potential targets. Note that no accumulation of the unconjugated coumarin **21** in any specific compartment was observed. To further analyze the subcellular localization of **5**, HeLa cells were treated with **5** and specific fluorescent probes for the mitochondria (Mitotracker), the endoplasmic reticulum (ER-tracker) and the endoplasmic reticulum (ER), and Golgi apparatus (BODIPY-brefeldin A). There was no colocalization of **5** with the mitochondrial marker (Figure 7A). In contrast, a clear overlap of both **5** and ER-specific probes was found (Figure 7B,C). These results suggest that **5** accumulates in the ER and that the molecular target of **5** should reside in the ER rather than in another subcellular localization.

Compound 3 Induces the Translocation of AIF and Caspase-12 to the Nucleus. Apoptosis inducing factor (AIF) is a mitochondrial protein that can induce apoptosis in a caspase-independent manner.[35] Upon an excessive calcium influx, AIF is cleaved by μ-calpain, released in the cytosol, and translocates to the nucleus where it induces chromatin

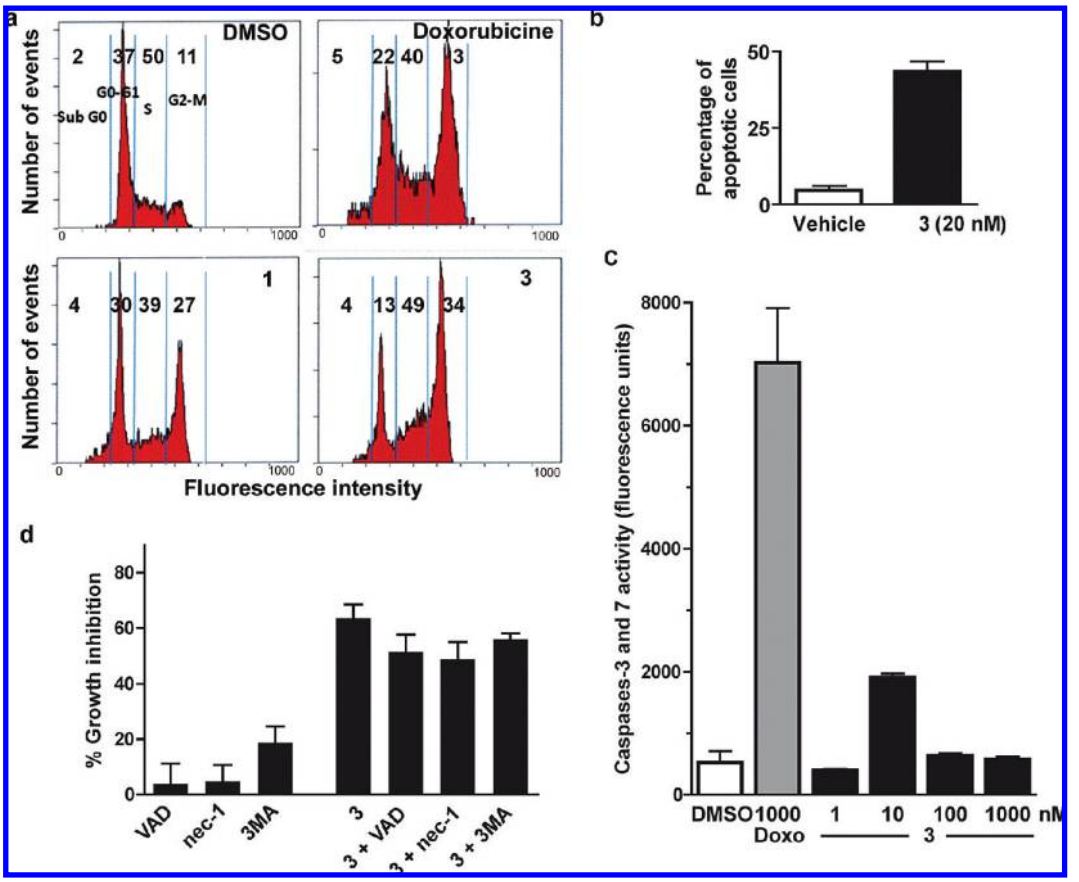

Figure 4. Compound **3** blocks HL60 cells in G2/M phase and induces apoptosis in a caspase-independent manner. (a) Blockade of HL60 cell cycle progression by **1** and **3**. HL60 cells were treated with doxorubicin (20 nM), **1** (200 nM), and **3** (20 nM) for 48 h. Cells were stained with propidium iodide, and the cell cycle distribution was determined using FACS ($n = 4$, each sample was duplicated). (b) Compound **3** induces apoptosis in HL60 cells. HL60 cells were treated with **3** (20 nM) for 72 h and apoptosis was quantified by staining with annexin V followed by flow cytometry. (c) Compound **3** (10^{-9}–10^{-6} M) does not activate caspases-3/7 in HL60 cells. HL60 cells were treated with **1**, **3**, or doxorubicine as a positive control, for 48 h. Whole cell extracts were prepared and assayed for their ability to cleave the caspase-3-specific substrate (DEVD-AMC). Relative fluorescence release was measured spectroscopically. Reaction rates were calculated from the slope of the linear time-dependent reaction and expressed as the fold-activation over the control (HL60 with DMSO alone). (d) Inhibitors of caspases, necroptosis and autophagy do not block the antiproliferative effects of **1** and **3** in HL60 cells. HL60 cells were treated for 72 h with **1**, **3**, or vehicle in the presence or not of Z-VAD-FMK (50 μM), necrostatin-1 (50 μM), and 3-methyladenine (2 mM), which inhibit caspases, autophagy, and necroptosis, respectively. Growth inhibition was not significantly altered by any of these inhibitors.

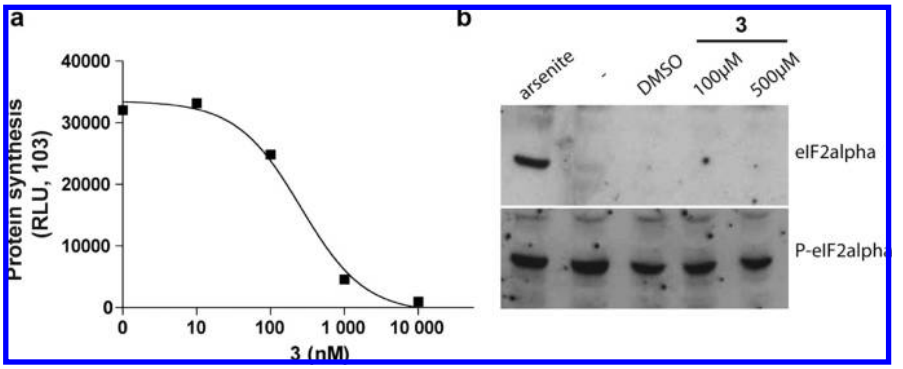

Figure 5. Compound **3** inhibits protein synthesis, independently from eIF2-α hosphorylation, at micromolar concentrations, i.e. at doses that are 3 orders of magnitude greater than those observed for cytotoxicity. (a) Compound **3** inhibits translation of capped and polyadenylated luciferase mRNA in a rabbit reticulocyte lysate (relative light units). Incubation time was 1 h. (b) Compound **3** does not induce the phosphorylation of eIF2-α in HeLa cells. Samples of total protein (10 μg) obtained from HeLa cells that were untreated, treated for 1 h with arsenite (500 μM), DMSO (vehicle), or **3** (100 or 500 μM) were analyzed by Western blotting with anti-eIF2-α and antiphospho-eIF2-α antibodies.

condensation and DNA fragmentation.[36] We analyzed by Western blot the effect of **3** on the localization of AIF in HL60 cells (Figure 8). Note that total AIF level remained unchanged upon **5** treatment. In nontreated cells, AIF was exclusively detected in the mitochondrial fraction. By comparison, after treatment with 20 nM **3** for 72 h, AIF was located mainly in the nucleus, indicating that in these cells, flavaglines induce apoptosis through the translocation of

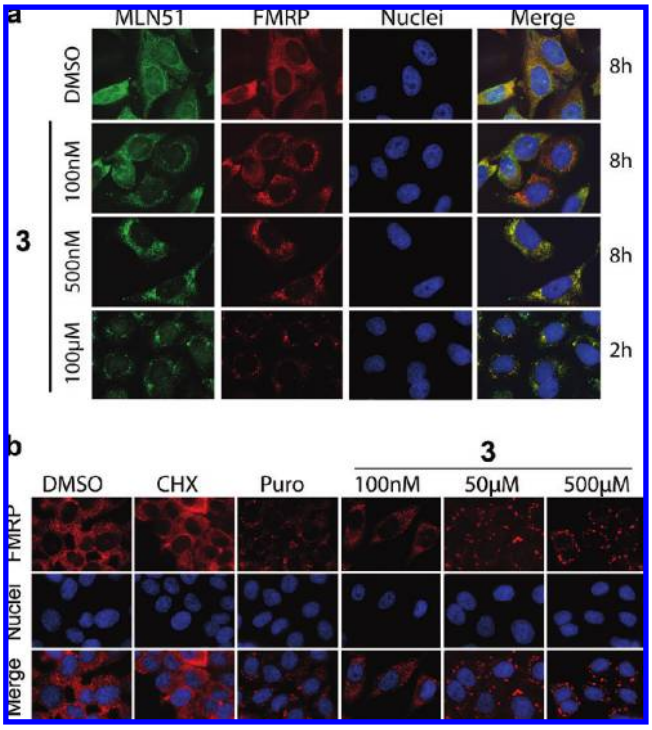

Figure 6. High concentrations of **3** induce the formation of stress granules in HeLa cells. (a) Immunofluorescence analysis of the stress-granules markers MLN51 and FMRP in HeLa cells after treatment with **3**. Cells were colabeled with anti-MLN51 (green) and anti-FMRP (red) antibodies. Treatment times are indicated on the right in hours (h). (b) Immunofluorescence analysis of HeLa cells treated with DMSO, cycloheximide (CHX; 10 μg/mL), puromycin (Puro; 100 μg/mL), or **3** (50, 100, or 500 μM) for 1 h. Immunofluorescence was assessed with an antibody to FMRP, a marker of stress granules. Cells were stained with an anti-FMRP antibody (red) and nuclei were counterstained with Hoechst 33258 (blue). Note that **3** induced the formation of stress granules at 50 μM, which is a concentration 10000 times higher than the effective cytotoxic doses. The protein synthesis inhibitors cycloheximide and puromycine were used as positive controls.

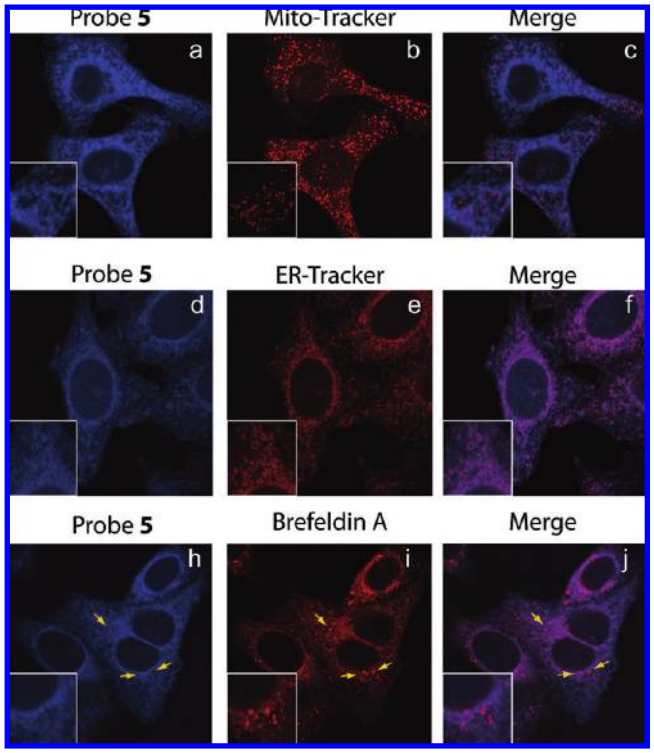

Figure 7. Subcellular localization of probe **5**. Upper panel, HeLa cells were treated with 50 μM of probe **5** (a, blue) for 2 h and 15 min with 1 μM of Mito-Tracker Red dye (b, red). Merged confocal image (c) shows that **5** does not localize in mitochondria. Middle panel, HeLa cells were treated with 50 μM of **5** (d, blue) for 2 h and 15 min with 1 μM of ER-tracker dye (e, red). Merge image (f) shows colocalization of both signals. Lower panel, HeLa cells were treated with 50 μM of **5** (h, blue) for 2 h and 15 min with 1 μM of BODIPY 558/568 brefeldin A (i, red), merge image (j) shows colocalization **5** and the brefeldin A-ER signal and not with the brefeldin A-Golgi signal. ER-tracker red dye and BODIPY 558/568 are selective for the endoplasmic reticulum (ER) and both the ER and Golgi apparatus, respectively. Merged confocal images show that probe **5** colocalizes with ER but not with the Golgi apparatus (yellow arrows). Inserts in the lower left corner of each image show a 2-fold magnification. Note that probe **5** does not localize in punctuate cytoplasmic foci like stress granules. Control probe **21** (unconjugated coumarin) gave no signal (not shown).

AIF to the nucleus. We then examined by immunohistochemistry whether **3** activates AIF in another human cancer cell line, and whether it also induces the translocation of caspase-12 from the ER to the nucleus, because this pro-apoptotic protein is involved in a cross-talk with AIF in ER stress-induced apoptosis.[35,37−39] In Hela cells treated with the vehicle only, antibodies specific to AIF or caspase-12 diffusely stained the perinuclear region of the cytoplasm. In contrast, in Hela cells treated with **3** (50 nM) for 72 h, these antibodies stained specifically the nucleus. The nuclear localization of AIF and caspase-12 was confirmed by co-staining with DAPI.

Next we examined the role of caspase-12 and of its activator, calpain, in the cytotoxicity of **3** in HL60 cells utilizing inhibitors of these enzymes. Caspase-12 inhibitor ATAD (Figure 8c) partially but significantly decreases the cytotoxicity of **3** (20 nM) in HL60 cells. It is noteworthy that ATAD itself displays some cytotoxicity in HL60 cells. These data indicate that caspase-12 is partially involved in **3**-induced apoptosis in HL60 cells. We did not observe any diminution of **3** cytotoxicity in presence of m-calpain inhibitor *N*-acetyl-Leu-Leu-methioninal, probably because of the intrinsic cytotoxicity of this compound. All together these data suggest that **3** may induce apoptosis through two independent pathways that involve AIF and caspase-12.

Discussion

All previously reported structure−activity relationships of flavaglines were performed with natural compounds extracted from plants. Modifications of the configuration of substituent at C-1, C-2, C-3, and C-3a positions, and methylation of the OH group at C-1, abolished cytostatic or cytotoxic activity, whereas substitution at C-2 by esters or amide groups is well tolerated (a more exhaustive presentation of the structure−activity relationships is reviewed in refs 1 and 2). Our present study extends this knowledge by showing that replacement of an electron-donating methoxy (R^1 = OMe) by a more lipophilic bromide significantly improves the cytotoxic potential. The cognate compound **3** displays a cytotoxicity that is at least 10 times more potent than those of doxorubicin, docetaxel, cisplatin, camptothecin, or vinblastine on a variety of human cancer cell lines.

Flavaglines derivatives **1** and **3** offer important advantages as antineoplastic agents. Flavaglines **1** and **3** are cytotoxic at

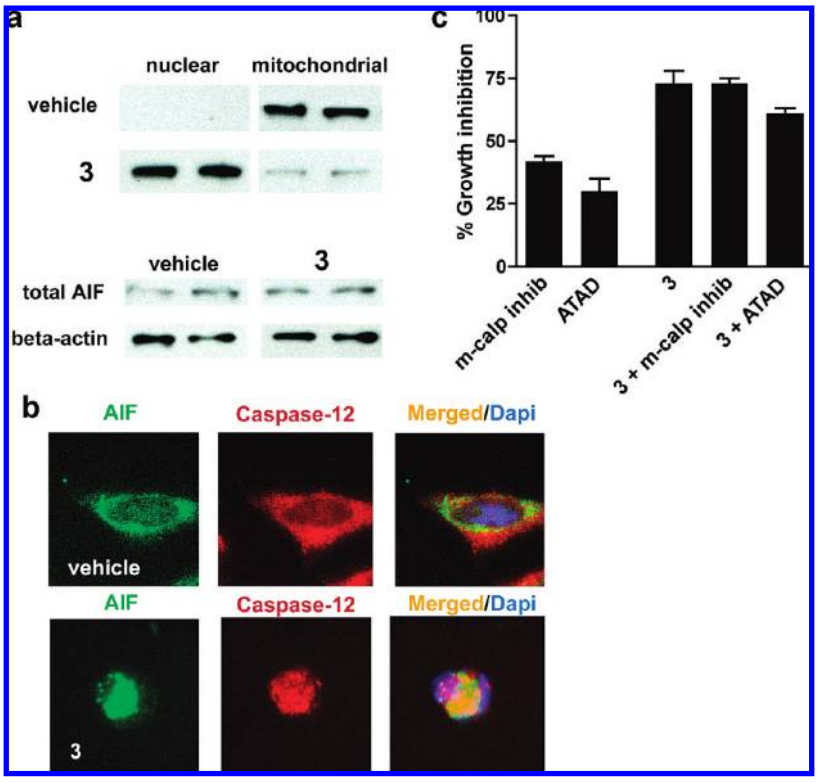

Figure 8. Compound **3** induces the translocation of AIF and caspase-12 to the nucleus. (a) After a 72 h treatment with **3** (20 nM) or its vehicle, HL60 cells were subjected to subcellular fractionation, and immunoblotting was performed with nuclear and mitochondrial fractions. β-Actin was used as an internal control. (b) Immunocytochemistry of AIF and caspase-12 in Hela cells treated for 72 h with **3** (50 nM) or its vehicle. Cells were colabeled with anti-AIF (green) and anti-caspase-12 (red) antibodies. Nuclei were stained by DAPI. (c) Inhibition of caspase-12 partially but significantly decreases the cytotoxicity of **3** in HL60 cells. HL60 cells were treated for 72 h with **3** (10 nM) or its vehicle in the presence or not of m-calpain inhibitor (20 μM) and caspase-12 inhibitor ATAD (10 μM).

concentrations in the nanomolar range, they seem insensitive to the acquired MDR1-resistance in MCF7R cell, and they act synergistically with anthracyclines in HepG2 cells. These observations are reminiscent of Stockwell's recent report that other inhibitors of protein synthesis (cycloheximide, emetine, and dihydrolycorine) also potentiate doxorubicin's lethality.[40] Moreover, combined treatment with **1** or **3** and doxorubicin showed a cumulative cytotoxic effect on HepG2 cells, indicating that flavaglines could be added to existing antineoplastic treatments. Another important feature of flavaglines is their absence of cardiotoxicity, which often occurs with anticancer drugs and which is the main limitation to the clinical use of anthracyclines.

Except for silvestrol and episilvestrol that have the peculiarity of a complex dioxanyl ring, flavaglines are generally considered to be cytostatic rather than cytotoxic.[4−8] However, here we found that flavaglines display a strong cytotoxicity toward many cancer cell lines. We showed that **1** and **3** block the cell cycle in phase G2/M, which is consistent with previous reports indicating that flavaglines cause dose-dependent G2/M phase arrest of various cancerous cell lines.[5,6,11] This G2/M cell cycle arrest is associated with the intrinsic apoptosis pathway and is induced by many other clinically used cytotoxic drugs.[38,39] Consistent with this finding, we found that the cytotoxic effect of **1** and **3** is due to induction of apoptosis in HL60 cells. Surprisingly, caspase assays indicated that caspases 3/7 were not specifically activated. This was confirmed by the observation that the broad caspase inhibitor Z-VAD-FMK did not alter the cytotoxicity of these compounds. The weak induction of caspases 3/7 and the absence of an effect in HeLa cells on caspases 8 and 9 by **1** and **3** are reminiscent of Kinghorn and Marian's observation that natural flavaglines silvestrol and aglaiastatin induce apoptosis without activating caspase-3 in SW480 and LNCap cells.[6,10] In contrast, Swanson showed that rocaglaol (nonracemic **1**) increased the level of cleaved caspase-7 and induced the intrinsic apoptotic pathway in the same LNCap cell line.[11] This discrepancy may be due either to a genetic instability and divergence of LNCap cells or to the fact that silvestrol and aglaiastatin do not act through the same molecular targets as rocaglaol. Also in contrast with our findings, Li-Weber reported that rocaglamide induces caspases 2, 3, 8, and 9 and triggers apoptosis through the intrinsic pathway in several leukemia cell lines isolated from patients.[14] These data clearly indicate that flavaglines may trigger apoptosis by different pathways according to the cancer cell types and may also be from the chemical structure of the drug.

Although the role of apoptosis in the cytotoxicity of anticancer drugs is well established, it is now evident that alternative forms of regulated cell death, such as autophagy or necroptosis, may also be involved.[41,42] Necroptosis occurs when a death receptor, such as Fas/CD95, TNFR1, death receptor (DR)4, and DR5, has been activated (e.g., by TNF-α) in the presence of a broad spectrum caspase inhibitor such as Z-VAD-FMK.[27] This form of death is characterized by necrotic cell death morphology and activation of autophagy. Necrostatin-1, which blocks necroptosis by inhibiting the adaptor kinase RIP1,[43] has been shown to prevent the death of MCF-7 and HEK293 cells induced by shikonin, a naturally occurring cytotoxic naphthoquinone.[44] Similarly, 3-methyla-

denine, an inhibitor of autophagy reduced the cytotoxicity of the anticancer drug etoposide in CaSki cells.[45] In our case, the cytotoxicity of **3** in HL60 was not reduced by Z-VAD-FMK, necrostatin-1, or 3-methyladenine, which indicates that, in these cells, flavaglines do not induce autophagy or necroptosis. However, we showed for the first time that flavagline **3** induces the death of HL60 and Hela cells via activation of the AIF and caspase-12 pathways, suggesting that **3** induces a stress in the ER.[35−39] This hypothesis is supported by the localization of probe **5** in the ER and by the formation of stress granules induced by **3**, albeit at high concentration. The ER fulfills specialized functions that are critical to the cell (protein translation and maturation, lipid synthesis, Ca^{2+} storage, and so on), thus, a dysregulation of ER homeostasis may jeopardize cell survival. It is now established that cross-talk between ER and mitochondria is decisive to commit the cell to apoptosis.[46,47] Marigo and collaborators have shown that ER stress in response to protein misfolding or disruptions of Ca^{2+} homeostasis activates at the same time AIF and caspase-12 apoptotic pathways in fibroblasts and models of retinitis pigmentosa.[38,39] Interestingly, both of these pathways were shown to reinforce each other.

The action of AIF has been shown to be critical for the cytotoxicity of other anticancer agents, such as arsenic trioxide for cervical cancer cells,[49] cisplatin for LNCaP prostate cancer cells,[50] taxol for SKOV3 ovarian carcinoma cells,[51] and flavopiridol for murine glioma cells.[52] More importantly, activation of AIF signaling by staurosporine induces cell death of nonsmall-cell lung carcinoma cells, which are highly resistant to conventional anticancer treatments.[53] Similarly, phytosphingosine treatment reversed the resistance of human T-cell lymphoma to gamma-radiation by induction of AIF-mediated apoptosis.[54] Caspase-12 has been shown to play a pivotal role in the induction of apoptosis by geldanamycin in BC-8 histiocytoma cells[48] and cisplatin in LLCPK renal epithelial cells.[55] Interestingly, VR3848, a novel cytotoxic cycloheptapeptide, has been recently shown to induce apoptosis in MCF-7 cells also through simultaneous stimulation of AIF and caspase-12 pathways.[56]

Previous studies showed that flavaglines are cytostatic or cytotoxic on all cancer cell lines tested, which suggests that the molecular target of these drugs is ubiquitous and that it affects a fundamental cellular pathway whose downstream effects lead to growth arrest or cell death in cancer cells. We found that **3** at high concentration induces stress granules and inhibits protein synthesis. Very recently, Pelletier and colleagues have shown that two naturally occurring flavaglines target protein synthesis through the translation initiation factor eIF4A by increasing its binding to RNA, thereby causing its sequestration and inhibiting cap-dependent translation.[34] These authors showed in particular that silvestrol and 1-*O*-formylaglafoline, two natural flavaglines, inhibit cap-dependent translation of firefly luciferase in vitro in cell-free Krebs-2 extracts, with IC_{50}s of 0.3 and 3 μM. In a similar assay we observed that **3** inhibited translation in reticulocyte lysates at comparable concentrations, with an IC_{50} of 0.2 μM. We also showed that inhibition of protein synthesis at the high concentration of **3** was not due to the phosphorylation of the eukaryotic initiation factor 2α (eIF-2α), consistent with the findings of Pelletier and colleagues, obtained for other flavaglines. However, pull-down experiments with immobilized ligand **6** suggested that flavaglines probably do not bind directly to eIF4A or that this binding requires another partner, such as mRNA or a scaffold protein.

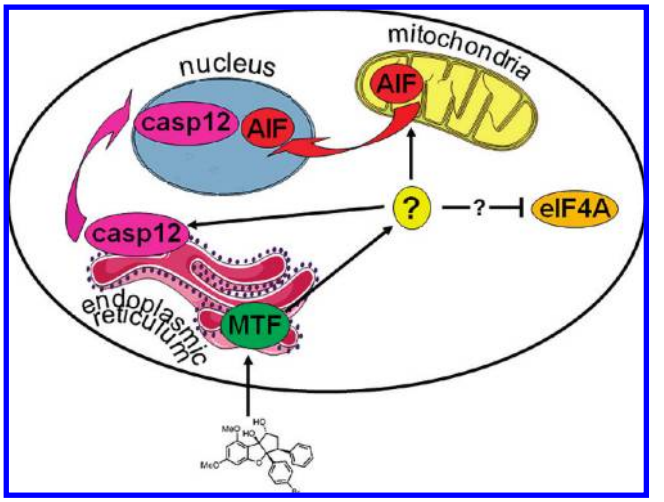

Figure 9. Proposed model for apoptosis induced by flavaglines in cancer cells. The binding to the molecular target of flavaglines (MTF) located in the ER triggers a cascade of events that lead to translocation of AIF and caspase-12 to the nucleus and also to inhibition of eIF4A.

Our microscopy data with probe **5** suggest that flavaglines might act on an ER component. The ER is the site of synthesis for glycoproteins and also membrane-bound and secreted proteins, which suggests that **3** may impair protein synthesis at the ER. It is therefore tempting to hypothesize that the binding of flavaglines to a target located in the ER may induce apoptosis in cancer cells through a cascade of events that include the translocation of AIF and caspase-12 to the nucleus and inhibition of eIF4A (Figure 9). The detailed molecular mechanism underlying flavagline cytotoxicity is currently under investigation.

Conclusion

We demonstrated for the first time that a flavagline (**3**) induces the death of cancer cells via activation of the AIF and caspase-12 pathways. This compound offers important advantages as antineoplastic agents. First, it is cytotoxic at concentrations in the nanomolar range on cancer cells but not on cardiomyocytes. Second, it is insensitive to the acquired MDR1-resistance in MCF7R cells. And third, it acts synergistically with anthracyclines independently of caspases-3, -7, -8, and -9, suggesting that it would retain its activity in cells refractory to activation of these caspases.[57] Considering that drug resistance and side effects are the two major obstacles limiting the efficacy of cancer chemotherapy, our results reinforce the view that flavaglines hold considerable potential for the treatment of cancers.

Experimental Section

Chemistry. General Methods. All reagents and solvents for syntheses were purchased from Sigma-Aldrich, Fluka, or Acros and used without further purification. Reagent-grade solvents were purified and dried using standard methods. Reactions were carried out under an argon atmosphere using flame-dried glassware with magnetic stirring and degassed solvents. Column chromatography was carried out on silica gel 60 (Merck, 70−230 mesh). ^{1}H NMR spectra at 300 MHz and ^{13}C NMR spectra at 75 MHz were recorded with DPX 300 SY Bruker spectrometers with the deuterated solvent as the lock and residual solvent as the internal reference. Infrared spectra were recorded using a Perkin-Elmer 881. Purity of target compounds were over

95% based on reversed-phase HPLC analyses (Hypersil Gold column 30 × 1 mm, C18) under the following conditions: flow rate: 0.3 mL/min; buffer A: CH_3CN, buffer B: 0.01% aqueous TFA; gradient: 98−10% buffer B over 8 min (detection: $\lambda = 220/254$ nm).

3-(2-(4-Bromophenyl)-2,3-dihydro-4,6-dimethoxy-3-oxobenzofuran-2-yl)-3-phenylpropanal (9c). A suspension of benzofuranone **7** (R^1 = Br, 4.7 g, 13.5 mmol) in *t*-BuOH (300 mL) was heated to 50 °C under argon. Benzyltrimethylammonium hydroxide in MeOH (40%, 306 μL, 0.73 mmol) and, immediately after, cinnamaldehyde **8** (3.40 mL, 27.0 mmol) were added. The mixture was stirred for 2 h at 50 °C, cooled to rt, concentrated and acidified with 1 M HCl (30 mL), extracted with CH_2Cl_2, dried over $MgSO_4$, and concentrated to dryness. Purification of the resulting yellow solid residue by chromatography (Et_2O−pentane 6:4) yielded 1.94 g (33%) of ketoaldehyde **9c** as a white solid: R_f 0.4 (Et_2O/hept 9:1). ^{1}H NMR ($CDCl_3$): 2.61 (1H, ddd, J = 0.9, 4.0, 17.3 Hz), 3.07 (1H, ddd, J = 2.3, 10.9, 17.3 Hz), 3.70 (3H, s), 3.85 (3H, s), 4.19 (1H, dd, J = 4.0, 10.9 Hz), 5.81 (1H, d, J = 1.8 Hz), 6.21 (1H, d, J = 1.8 Hz), 7.08−7.17 (3H, m), 7.29−7.32 (2H, m), 7.49, 7.63 (4H, AA′BB′, J = 8.7 Hz), 9.41 (1H, d, J = 1.1 Hz). ^{13}C NMR ($CDCl_3$): 44.0, 46.8, 55.9, 55.9, 88.4, 93.0, 103.7, 122.6, 126.9, 127.5, 128.2, 129.5, 131.8, 132.0, 135.6, 136.3, 159.1, 169.9, 174.1, 194.1, 200.0. IR (thin film): 2725, 1720, 1699, 1617, 1590, 1154, 747 cm^{-1}. HR-MS calcd for $C_{25}H_{21}BrLiO_5$, 487.0732; found, 487.0727.

3a-(4-Bromophenyl)-6,8-dimethoxy-8b-hydroxy-3-phenyl-2,3−3a,8b-tetrahydro-cyclopenta[*b*]benzofuran-1-one (12c). Trimethylsilyl cyanide (744 mg, 7.5 mmol) was added dropwise to a solution of aldehyde **9c** (1.2 g, 2.5 mmol) in CH_3CN (12 mL) at room temperature under argon. Immediately after, zinc iodide (10 mg) was added, and the resulting mixture was stirred for 1 h, filtered, and concentrated to afford crude cyanohydrin **11c** (1.74 g, 40%), which was used in the next step without purification. LDA (2.7 mmol, 0.6 M) in THF was added dropwise at −78 °C under argon to a solution of cyanohydrin **11c** (1.43 g, 2.46 mmol) in dry THF (12 mL). After stirring for 2 h at −78 °C, the solution was heated to −50 °C for 10 min. The reaction was quenched by the addition of saturated aqueous ammonium chloride (15 mL). Standard extractive workup (CH_2Cl_2) gave a yellow solid (1.49 g). This solid was directly treated with tetra-*n*-butylammonium fluoride (2.7 mL, 1 M in THF) added dropwise at room temperature in dry THF (10 mL). The solution was stirred for 4 h and quenched by addition of methanol. Standard extractive workup (AcOEt) and purification by flash chromatography (Et_2O) afforded tricyclic ketone **12c** (240 mg, 20%) as a white solid: R_f 0.35 (Et_2O/hept 8:2). ^{1}H NMR ($CDCl_3$): 2.96−3.09 (2H, m), 3.21 (1H, br s), 3.81 (3H, s), 3.84 (3H, s), 3.90 (1H, dd, J = 10.2, 12.1 Hz), 6.10 (1H, d, J = 1.9 Hz), 6.33 (1H, d, J = 1.9 Hz), 6.89−6.94 (4H, m), 7.10−7.12 (3H, m), 7.24−7.27 (2H, m). ^{13}C NMR ($CDCl_3$): 39.6, 48.6, 55.6, 55.7, 88.6, 89.7, 92.8, 100.8, 106.2, 121.7, 127.1, 127.8, 128.0, 128.3, 130.7, 133.0, 136.6, 158.4, 160.9, 164.8, 210.3. IR (thin film): 3477, 2942, 2841, 1750, 1621, 1597, 1149 cm^{-1}. HR-MS calcd for $C_{25}H_{21}Br_1Na_1O_6$, 503.0470; found, 503.0465.

3a-(4-Bromophenyl)-6,8-dimethoxy-3-phenyl-1,2,3,3a-tetrahydro-cyclopenta[*b*]benzofuran-1,8*b*(1*H*)-diol (3). CH_3CN (1.8 mL) was added at room temperature under argon to $Me_4NBH(OAc)_3$ (828 mg, 3.15 mmol) followed by the addition of glacial acetic acid (1.8 mL). After stirring for 30 min at room temperature a solution of ketone **12c** (170 mg, 0.354 mmol) in CH_3CN (4.5 mL) was added dropwise. The resulting mixture was stirred overnight at room temperature. The reaction was quenched by the addition of saturated aqueous ammonium chloride (40 mL). Standard extractive workup (AcOEt) and purification by flash chromatography (Et_2O) afforded **3** (103 mg, 60%) as a white solid: R_f 0.25 (Et_2O/hept 8:2). ^{1}H NMR ($CDCl_3$): 1.89 (1H, br s), 2.14 (1H, dd, J = 7.0, 13.3 Hz), 2.67 (1H, ddd, J = 6.4, 13.9, 13.9 Hz), 3.27 (1H, br s), 3.83 (3H, s), 3.86 (3H, s), 3.99 (1H, dd, J = 6.5, 14.0 Hz), 4.77 (1H, d, J = 6.0 Hz), 6.10 (1H, d, J = 1.8 Hz), 6.28 (1H, d, J = 1.8 Hz), 6.95−6.98 (2H, m), 7.05−7.12 (5H, m), 7.23−7.26 (2H, m). ^{13}C NMR ($CDCl_3$): 36.1, 53.2, 55.6, 55.7, 79.0, 89.4, 92.5, 94.8, 103.1, 107.4, 121.4, 126.4, 127.7, 127.9, 129.4, 130.2, 134.1, 138.1, 156.8, 160.6, 163.9. IR (thin film): 3486, 2942, 2841, 1624, 1598, 1147 cm^{-1}. HR-MS calcd for $C_{25}H_{23}Br_1K_1O_6$, 521.0366; found, 521.0360.

Biological Assay Methods. Materials. Necrostatin-1 was synthesized according to the procedure of Degterev et al.[27] 3-Methyladenine was purchased from Acros Organics, Z-VAD-FMK from Bachem, and ATAD from PromoCell. Rhodamine 123 and *N*-acetyl-Leu-Leu-methioninal were from Sigma and DEVD-AMC, LEHD-AMC, IETD-AMC, MG132, LLVY-AMC, and RLR-AMC were purchased from Biomol. Rabbit antiactive caspase-3 polyclonal antibody was bought from Chemicon International.

eIF2α Phosphorylation by Western Blotting. HeLa cells were treated or not with DMSO, sodium arsenite (500 μM), or **3** (100 and 500 μM) for 1 h. Cell lysates were employed to SDS-PAGE. The blots were incubated with horseradish peroxidase-conjugated (HRP) AffiniPure donkey antirabbit at 1/10000 (Jackson ImmunoResearch). Finally, protein−antibody complexes were visualized by an enhanced chemiluminescence detection system (ECL detection reagent, Amersham).

Detection of Stress-Granules by Immunofluorescence. HeLa cells were seeded on glass coverslips in 24-well plates in DMEM supplemented with 5% of fetal calf serum. After 24 h of culture, cells were treated with cycloheximide (10 μg/mL) or puromycin (100 μg/mL) for 1 h or with different concentrations of **3** (50 nM to 500 μM) for 30 min to 8 h and examined by immunofluorescence using rabbit anti-MLN51 and mouse anti-FMRP antibodies as previously described.[32] See Supporting Information for more details.

Preparation of Nuclear and Mitochondrial Fractions. HL60 cells (10^5) were seeded and treated with **3** (20 nM) or its vehicle (DMSO). After 72 h the cells were collected and washed with PBS, incubated on ice for 10 min, and then resuspended in isotonic homogenization buffer (250 mM sucrose, 10 mM KCl, 1.5 mM $MgCl_2$, 1 mM EDTA, 1 mM EGTA, 1 mM dithiothreitol, 10 mM Tris-HCl, pH 7.4, containing protease inhibitor mixture (Roche)). The cells were sonicated for 1 min at 30% amplitude. Unbroken cells were removed by centrifugation ($30 \times g$ for 5 min). Nuclei and mitochondrial fractions were separated by centrifugation at $750 \times g$ for 20 min and $14000 \times g$ for 30 min, respectively. The nuclear fraction was washed three times with 0.01% (v/v) NP40 containing isotonic homogenization buffer. The nuclear and mitochondrial fractions were then subjected to Western blot analysis with a rabbit anti-AIF polyclonal antibody (1: 500, Santa Cruz Biotechnology, U.S.A.).

Acknowledgment. This article is dedicated to our friend and mentor, Prof. Roger A. Johnson. Generous financial support for this work was provided to L.D. by the "Association pour la Recherche sur le Cancer" (ARC, grant #3940). We thank ARC (A.B.) and MNESR (F.T. and R.D.) for fellowships and Dr. Markus R. Dobler (Syngenta, Basel) for helpful discussions.

Supporting Information Available: Supplementary biological data (effect on the body weight in mice, cell cycle arrest in HL60 cells, activation of caspases 8 and 9, antiproliferative effects in presence of inhibitors of caspases, necroptosis, and autophagy, proteasome assay, and **6**-agarose pull-down assay), synthesis of compounds **1**, **2**, and **4**−**6**, and supplementary biological assay methods. This material is available free of charge via the Internet at http://pubs.acs.org.

References

(1) Kim, S.; Salim, A. A.; Swanson, S. M.; Kinghorn, A. D. Potential of cyclopenta[*b*]benzofurans from Aglaia species in cancer chemotherapy. *Anticancer Agents Med. Chem.* **2006**, *6*, 319–345.

(2) Proksch, P.; Edrada, R.; Ebel, R.; Bohnenstengel, F.; Nugroho, B. Chemistry and biological activity of rocaglamide derivatives and related compounds in *Aglaia* species (*Meliaceae*). *Curr. Org. Chem.* **2001**, *5*, 923–938.

(3) King, M. L.; Chiang, C. C.; Ling, H. C.; Fujita, E.; Ochiai, M.; McPhail, A. T. X-Ray crystal structure of rocaglamide, a novel antileukemic 1*H*-cyclopenta[*b*]benzofuran from *Aglaia elliptifolia*. *Chem. Commun.* **1992**, 1150–1151.

(4) Bohnenstengel, F. I.; Steube, K. G.; Meyer, C.; Nugroho, B. W.; Hung, P. D.; Kiet, L. C.; Proksch, P. Structure activity relationships of antiproliferative rocaglamide derivatives from *Aglaia* species (*Meliaceae*). *Z. Naturforsch., C: J. Biosci.* **1999**, *54*, 55–60.

(5) Bohnenstengel, F. I.; Steube, K. G.; Meyer, C.; Quentmeier, H.; Nugroho, B. W.; Proksch, P. 1*H*-Cyclopenta[*b*]benzofuran lignans from Aglaia species inhibit cell proliferation and alter cell cycle distribution in human monocytic leukemia cell lines. *Z. Naturforsch., C: J. Biosci.* **1999**, *54*, 1075–1083.

(6) Hausott, B.; Greger, H.; Marian, B. Flavaglines: a group of efficient growth inhibitors block cell cycle progression and induce apoptosis in colorectal cancer cells. *Int. J. Cancer* **2004**, *109*, 933–940.

(7) Lee, S. K.; Cui, B.; Mehta, R. R.; Kinghorn, A. D.; Pezzuto, J. M. Cytostatic mechanism and antitumor potential of novel 1*H*-cyclopenta[*b*]benzofuran lignans isolated from *Aglaia elliptica*. *Chem. Biol. Interact.* **1998**, *115*, 215–228.

(8) Ohse, T.; Ohba, S.; Yamamoto, T.; Koyano, T.; Umezawa, K. Cyclopentabenzofuran lignan protein synthesis inhibitors from *Aglaia odorata*. *J. Nat. Prod.* **1996**, *59*, 650–652.

(9) Cui, B.; Chai, H.; Santisuk, T.; Reutrakul, V.; Farnsworth, N. R.; Pezzuto, J. M.; Kinghorn, A. D. Novel cytotoxic 1*H*-cyclopenta-[*b*]benzofuran lignans from *Aglaia elliptica*. *Tetrahedron* **1997**, *53*, 17625–17632.

(10) Kim, S.; Hwang, B. Y.; Su, B. N.; Chai, H.; Mi, Q.; Kinghorn, A. D.; Wild, R.; Swanson, S. M. Silvestrol, a potential anticancer rocaglate derivative from *Aglaia foveolata*, induces apoptosis in LNCaP cells through the mitochondrial/apoptosome pathway without activation of executioner caspase-3 or -7. *Anticancer Res.* **2007**, *27*, 2175–2183.

(11) Mi, Q.; Su, B. N.; Chai, H.; Cordell, G. A.; Farnsworth, N. R.; Kinghorn, A. D.; Swanson, S. M. Rocaglaol induces apoptosis and cell cycle arrest in LNCaP cells. *Anticancer Res.* **2006**, *26*, 947–952.

(12) Wang, S. K.; Duh, C. Y. Cytotoxic cyclopenta[*b*]benzofuran derivatives from the stem bark of *Aglaia formosana*. *Planta Med.* **2001**, *67*, 555–557.

(13) Wu, T. S.; Liou, M. J.; Kuoh, C. S.; Teng, C. M.; Nagao, T.; Lee, K. H. Cytotoxic and antiplatelet aggregation principles from *Aglaia elliptifolia*. *J. Nat. Prod.* **1997**, *60*, 606–608.

(14) Zhu, J. Y.; Lavrik, I. N.; Mahlknecht, U.; Giaisi, M.; Proksch, P.; Krammer, P. H.; Li-Weber, M. The traditional Chinese herbal compound rocaglamide preferentially induces apoptosis in leukemia cells by modulation of mitogen-activated protein kinase activities. *Int. J. Cancer* **2007**, *121*, 1839–1846.

(15) Su, B. N.; Chai, H.; Mi, Q.; Riswan, S.; Kardono, L. B.; Afriastini, J. J.; Santarsiero, B. D.; Mesecar, A. D.; Farnsworth, N. R.; Cordell, G. A.; Swanson, S. M.; Kinghorn, A. D. Activity-guided isolation of cytotoxic constituents from the bark of *Aglaia crassinervia* collected in Indonesia. *Bioorg. Med. Chem.* **2006**, *14*, 960–972.

(16) Mi, Q.; Kim, S.; Hwang, B. Y.; Su, B. N.; Chai, H.; Arbieva, Z. H.; Kinghorn, A. D.; Swanson, S. M. Silvestrol regulates G2/M checkpoint genes independent of p53 activity. *Anticancer Res.* **2006**, *26*, 3349–3356.

(17) Dobler, M. R.; Bruce, I.; Cederbaum, F.; Cooke, N. G.; Diorazio, L. J.; Hall, R. G.; Irving, E. Total synthesis of (±)-rocaglamide and some aryl analogues. *Tetrahedron Lett.* **2001**, *42*, 8281–8284.

(18) Alexander, M. D.; Burkart, M. D.; Leonard, M. S.; Portonovo, P.; Liang, B.; Ding, X.; Joullie, M. M.; Gulledge, B. M.; Aggen, J. B.; Chamberlin, A. R.; Sandler, J.; Fenical, W.; Cui, J.; Gharpure, S. J.; Polosukhin, A.; Zhang, H. R.; Evans, P. A.; Richardson, A. D.; Harper, M. K.; Ireland, C. M.; Vong, B. G.; Brady, T. P.; Theodorakis, E. A.; La Clair, J. J. A central strategy for converting natural products into fluorescent probes. *ChemBioChem* **2006**, *7*, 409–416.

(19) Gerard, B.; Jones Ii, G.; Porco, J. A., Jr. A biomimetic approach to the rocaglamides employing photogeneration of oxidopyryliums derived from 3-hydroxyflavones. *J. Am. Chem. Soc.* **2004**, *126*, 13620–13621.

(20) Beer, P. D.; Cadman, J.; Lloris, J. M.; Martinez-Manez, R.; Soto, J.; Pardo, T.; Dolores Marcos, M. Anion interaction with ferrocene-functionalized cyclic and open-chain polyaza and aza-oxa cycloalkanes. *J. Chem. Soc., Dalton Trans.* **2000**, 1805–1812.

(21) Lee, J. W.; Fuchs, P. L. Reduction of azides to primary amines in substrates bearing labile ester functionality. Synthesis of a PEG-solubilized, "Y"-shaped iminodiacetic acid reagent for preparation of folate-tethered drugs. *Org. Lett.* **1999**, *1*, 179–181.

(22) Baumann, B.; Bohnenstengel, F.; Siegmund, D.; Wajant, H.; Weber, C.; Herr, I.; Debatin, K. M.; Proksch, P.; Wirth, T. Rocaglamide derivatives are potent inhibitors of NF-kappa B activation in T-cells. *J. Biol. Chem.* **2002**, *277*, 44791–44800.

(23) Levin, B.; Amos, C. Therapy of unresectable hepatocellular carcinoma. *N. Engl. J. Med.* **1995**, *332*, 1294–1296.

(24) Force, T.; Krause, D. S.; Van Etten, R. A. Molecular mechanisms of cardiotoxicity of tyrosine kinase inhibition. *Nat. Rev. Cancer* **2007**, *7*, 332–344.

(25) Sereno, M.; Brunello, A.; Chiappori, A.; Barriuso, J.; Casado, E.; Belda, C.; de Castro, J.; Feliu, J.; Gonzalez-Baron, M. Cardiac toxicity: old and new issues in anti-cancer drugs. *Clin. Transl. Oncol.* **2008**, *10*, 35–46.

(26) Sardao, V. A.; Oliveira, P. J.; Holy, J.; Oliveira, C. R.; Wallace, K. B. Morphological alterations induced by doxorubicin on H9c2 myoblasts: nuclear, mitochondrial, and cytoskeletal targets. *Cell. Biol. Toxicol.* **2009**, *25*, 227–243.

(27) Degterev, A.; Huang, Z.; Boyce, M.; Li, Y.; Jagtap, P.; Mizushima, N.; Cuny, G. D.; Mitchison, T. J.; Moskowitz, M. A.; Yuan, J. Chemical inhibitor of nonapoptotic cell death with therapeutic potential for ischemic brain injury. *Nat. Chem. Biol.* **2005**, *1*, 112–119.

(28) Seglen, P. O.; Gordon, P. B. 3-Methyladenine: specific inhibitor of autophagic/lysosomal protein degradation in isolated rat hepatocytes. *Proc. Natl. Acad. Sci. U.S.A.* **1982**, *79*, 1889–1892.

(29) Richardson, P. G.; Mitsiades, C.; Hideshima, T.; Anderson, K. C. Proteasome inhibition in the treatment of cancer. *Cell Cycle* **2005**, *4*, 290–296.

(30) Anderson, P.; Kedersha, N. Stress granules: the Tao of RNA triage. *Trends Biochem. Sci.* **2008**, *33*, 141–150.

(31) Donze, O.; Jagus, R.; Koromilas, A. E.; Hershey, J. W.; Sonenberg, N. Abrogation of translation initiation factor eIF-2 phosphorylation causes malignant transformation of NIH 3T3 cells. *EMBO J.* **1995**, *14*, 3828–3834.

(32) Baguet, A.; Degot, S.; Cougot, N.; Bertrand, E.; Chenard, M. P.; Wendling, C.; Kessler, P.; Le Hir, H.; Rio, M. C.; Tomasetto, C. The exon-junction-complex-component metastatic lymph node 51 functions in stress-granule assembly. *J. Cell Sci.* **2007**, *120*, 2774–2784.

(33) Mazroui, R.; Huot, M. E.; Tremblay, S.; Filion, C.; Labelle, Y.; Khandjian, E. W. Trapping of messenger RNA by fragile X mental retardation protein into cytoplasmic granules induces translation repression. *Hum. Mol. Genet.* **2002**, *11*, 3007–3017.

(34) Bordeleau, M. E.; Robert, F.; Gerard, B.; Lindqvist, L.; Chen, S. M.; Wendel, H. G.; Brem, B.; Greger, H.; Lowe, S. W.; Porco, J. A., Jr.; Pelletier, J. Therapeutic suppression of translation initiation modulates chemosensitivity in a mouse lymphoma model. *J. Clin. Invest.* **2008**, *118*, 2651–2660.

(35) Broker, L. E.; Kruyt, F. A.; Giaccone, G. Cell death independent of caspases: a review. *Clin. Cancer Res.* **2005**, *11*, 3155–3162.

(36) Modjtahedi, N.; Giordanetto, F.; Madeo, F.; Kroemer, G. Apoptosis-inducing factor: vital and lethal. *Trends Cell. Biol.* **2006**, *16*, 264–272.

(37) Nakagawa, T.; Zhu, H.; Morishima, N.; Li, E.; Xu, J.; Yankner, B. A.; Yuan, J. Caspase-12 mediates endoplasmic-reticulum-specific apoptosis and cytotoxicity by amyloid-β. *Nature* **2000**, *403*, 98–103.

(38) Sanges, D.; Comitato, A.; Tammaro, R.; Marigo, V. Apoptosis in retinal degeneration involves cross-talk between apoptosis-inducing factor (AIF) and caspase-12 and is blocked by calpain inhibitors. *Proc. Natl. Acad. Sci. U.S.A.* **2006**, *103*, 17366–17371.

(39) Sanges, D.; Marigo, V. Cross-talk between two apoptotic pathways activated by endoplasmic reticulum stress: differential contribution of caspase-12 and AIF. *Apoptosis* **2006**, *11*, 1629–1641.

(40) Smukste, I.; Bhalala, O.; Persico, M.; Stockwell, B. R. Using small molecules to overcome drug resistance induced by a viral oncogene. *Cancer Cell* **2006**, *9*, 133–146.

(41) Kim, R. Recent advances in understanding the cell death pathways activated by anticancer therapy. *Cancer* **2005**, *103*, 1551–1560.

(42) Ricci, M. S.; Zong, W. X. Chemotherapeutic approaches for targeting cell death pathways. *Oncologist* **2006**, *11*, 342–357.

(43) Degterev, A.; Hitomi, J.; Germscheid, M.; Ch'en, I. L.; Korkina, O.; Teng, X.; Abbott, D.; Cuny, G. D.; Yuan, C.; Wagner, G.; Hedrick, S. M.; Gerber, S. A.; Lugovskoy, A.; Yuan, J. Identification of RIP1 kinase as a specific cellular target of necrostatins. *Nat. Chem. Biol.* **2008**, *4*, 313–321.

(44) Han, W.; Li, L.; Qiu, S.; Lu, Q.; Pan, Q.; Gu, Y.; Luo, J.; Hu, X. Shikonin circumvents cancer drug resistance by induction of a necroptotic death. *Mol. Cancer Ther.* **2007**, *6*, 1641–1649.

(45) Lee, S. B.; Tong, S. Y.; Kim, J. J.; Um, S. J.; Park, J. S. Caspase-independent autophagic cytotoxicity in etoposide-treated CaSki cervical carcinoma cells. *DNA Cell Biol.* **2007**, *26*, 713–720.
(46) Heath-Engel, H. M.; Chang, N. C.; Shore, G. C. The endoplasmic reticulum in apoptosis and autophagy: role of the BCL-2 protein family. *Oncogene* **2008**, *27*, 6419–6433.
(47) Madeo, F.; Kroemer, G. Intricate links between ER stress and apoptosis. *Mol. Cell* **2009**, *33*, 669–670.
(48) Taiyab, A.; Sreedhar, A. S.; Rao Ch, M. Hsp90 inhibitors, GA and 17AAG, lead to ER stress-induced apoptosis in rat histiocytoma. *Biochem. Pharmacol.* **2009**, *78*, 142–152.
(49) Kang, Y. H.; Yi, M. J.; Kim, M. J.; Park, M. T.; Bae, S.; Kang, C. M.; Cho, C. K.; Park, I. C.; Park, M. J.; Rhee, C. H.; Hong, S. I.; Chung, H. Y.; Lee, Y. S.; Lee, S. J. Caspase-independent cell death by arsenic trioxide in human cervical cancer cells: reactive oxygen species-mediated poly(ADP-ribose) polymerase-1 activation signals apoptosis-inducing factor release from mitochondria. *Cancer Res.* **2004**, *64*, 8960–8967.
(50) Zhang, W.; Zhang, C.; Narayani, N.; Du, C.; Balaji, K. C. Nuclear translocation of apoptosis inducing factor is associated with cisplatin induced apoptosis in LNCaP prostate cancer cells. *Cancer Lett.* **2007**, *255*, 127–134.
(51) Ahn, H. J.; Kim, Y. S.; Kim, J. U.; Han, S. M.; Shin, J. W.; Yang, H. O. Mechanism of taxol-induced apoptosis in human SKOV3 ovarian carcinoma cells. *J. Cell Biochem.* **2004**, *91*, 1043–1052.
(52) Newcomb, E. W.; Tamasdan, C.; Entzminger, Y.; Alonso, J.; Friedlander, D.; Crisan, D.; Miller, D. C.; Zagzag, D. Flavopiridol induces mitochondrial-mediated apoptosis in murine glioma GL261 cells via release of cytochrome c and apoptosis inducing factor. *Cell Cycle* **2003**, *2*, 243–250.
(53) Gallego, M. A.; Joseph, B.; Hemstrom, T. H.; Tamiji, S.; Mortier, L.; Kroemer, G.; Formstecher, P.; Zhivotovsky, B.; Marchetti, P. Apoptosis-inducing factor determines the chemoresistance of non-small-cell lung carcinomas. *Oncogene* **2004**, *23*, 6282–6291.
(54) Park, M. T.; Kim, M. J.; Kang, Y. H.; Choi, S. Y.; Lee, J. H.; Choi, J. A.; Kang, C. M.; Cho, C. K.; Kang, S.; Bae, S.; Lee, Y. S.; Chung, H. Y.; Lee, S. J. Phytosphingosine in combination with ionizing radiation enhances apoptotic cell death in radiation-resistant cancer cells through ROS-dependent and -independent AIF release. *Blood* **2005**, *105*, 1724–1733.
(55) Liu, H.; Baliga, R. Endoplasmic reticulum stress-associated caspase 12 mediates cisplatin-induced LLC-PK1 cell apoptosis. *J. Am. Soc. Nephrol.* **2005**, *16*, 1985–1992.
(56) Ubol, S.; Kramyu, J.; Masrinoul, P.; Kachangchaeng, C.; Pittayanurak, P.; Sophasan, S.; Reutrakul, V. A novel cycloheptapeptide exerts strong anticancer activity via stimulation of multiple apoptotic pathways in caspase-3 deficient cancer cells. *Anticancer Res.* **2007**, *27*, 2473–2479.
(57) Lorenzo, H. K.; Susin, S. A. Therapeutic potential of AIF-mediated caspase-independent programmed cell death. *Drug Resist. Updates* **2007**, *10*, 235–255.